2022

The Effects of the Orientation of Outdoor Microchannel Heat Exchanger on the Performance of a Transcritical R744 Heat Pump During Frosting and Defrosting

Wenying Zhang

Pega Hrnjak

The Effects of the Orientation of Outdoor Microchannel Heat Exchanger on the Performance of a Transcritical R744 Heat Pump During Frosting and Defrosting

Wenying ZHANG [1], Pega HRNJAK[1, 2]*

[1]ACRC, University of Illinois, Urbana, Illinois, USA
wenying3@illinois.edu

[2]Creative Thermal Solutions, Inc., Urbana, Illinois, USA
pega@illinois.edu

* Corresponding Author

ABSTRACT

This paper presents the transient performance of a transcritical R744 heat pump (HP) system with a horizontally and vertically oriented outdoor microchannel heat exchanger during continuous frosting and defrosting cycles. The refrigerant migration, heating capacity, efficiency degradation during the frosting process, and the water retention after defrosting are presented and discussed. The frosting and defrosting functions were monitored using three web cameras to understand better the refrigerant and frost distribution on the two-pass outdoor coil. The results show that the vertically oriented outdoor coil improves heat pump performance both in frosting and defrosting due to better distribution of two-phase refrigerant and water drainage.

1. INTRODUCTION

In recent decades, electric vehicles (EVs) have been promoted in many countries to reduce air pollution and limit climate change. Despite the rapid growth of the EV market, EVs still face the challenge of range anxiety in cold weather. One way to help is to use the air-conditioning system in reverse mode, as a heat pump and that way reduces the draw of electricity from the battery. By improving frosting/defrosting efficiency, and condensate removal for the outdoor evaporator, the efficiency of the heat pump can be increased. Frost grows on the outdoor evaporator when its surface temperature is lower than both the freezing point of water and the dew point temperature during the operation.

In the earlier stage, researchers studied the fundamental aspects of frosting- the different phases of frost growth, the properties of frost, and the effects of environmental conditions. Hayashi et al. (1977) classified the frost formation types on a cold plate in the temperature range of 0 to -25°C and humidity range of 0.002 to 0.010 $kg/kg_{dry,air}$ in forced convection. The map of the frost types was developed and divided based on humidity and the cold plate temperature. Also, the density and effective thermal conductivity were studied and related to the frost formation types. But the authors focus on the growth process of the frost layer, while the nucleation process was not well discussed. Na and Webb (2003) analyzed the nucleation process theoretically for the incipient frost formation and concluded that the air at the cold surface should be supersaturated for frost formation to start. Also, lower energy surfaces (high contact angle) require a higher supersaturation degree for nucleation, while surface roughness reduces the required supersaturation degree. The authors also validated their conclusions with experiments using five different kinds of surfaces. Yang and Lee (2004) conducted experiments to obtain the impact of various environmental parameters on the properties of frost formed on a cold plate. The range of the test conditions is the following: the air temperature of 5 to 15°C, air velocity of 1.0 to 2.5 m/s, absolute humidity of 0.0032 to 0.0085 $kg/kg_{dry\ air}$, and cold plate temperature of -35 to -15°C. The thickness, density, surface temperature, thermal conductivity, and average heat and mass transfer coefficient of the frost layer were correlated as functions of Re number, Fourier number, absolute humidity, and dimensionless temperature. However, the air inlet temperatures for this study are above 5°C and the relative humidity are lower than 80%, which might not be the most common weather in winter. Therefore, studies under the conditions of automobile or residential air-source heat pump with sub-freezing air temperatures required further exploration.

In addition to the fundamental studies, researchers have explored different engineering methods to address the frosting issue of the Air-Source Heat Pump (ASHP). Passive methods employ different designs of the geometry of outdoor heat exchangers, system architecture, and surface features to slow the frost growing on the outdoor coil. Zhang and Hrnjak (2009) experimentally compared three types of heat exchangers: conventional round tube plate fin (RTPF), flat tube with parallel flow serpentine fin (PFSF), and new design of parallel flow plate-fin (PF^2). The frosting conditions were the following: the air temperature of 0℃, the coolant inlet temperature of -14.5℃, the initial air inlet velocity of 0.9, 2, 3 m/s, and relative humidity of 70 and 80%. The data showed that the RTPF heat exchanger has the longest frosting time due to the two times large air-side surface area. The frost accumulation speed is slower for the PF^2 than it is for PFSF, and the orientation has negligible effects on the performance of PF^2 heat exchanger. The authors also experimentally studied the effects of louver angles (15, 27, and 39 deg) and fin pitches (12, 15, and 18 fpi) on the pressure drop and overall heat transfer coefficient of serpentine fin microchannel heat exchangers in periodic frosting (Hrnjak et al., 2017). The combination of 18 fpi and 39˚ had the highest overall heat transfer coefficient and the most desirable pressure drop due to the best drainage, although it was not good in dry conditions. Also, several (4 to 8) repetitive frosting/defrosting cycles were necessary to reach the saturation in water retention and the performance in real operation. However, both studies focus on the performance of heat exchangers only, while the effects of frosting and defrosting on the performance of ASHP systems were not discussed. On the other hand, improving the system architecture can increase the evaporating temperature and therefore improve the performance of the heat pump in frosting conditions. Cernicin et al. (2022) investigated the effects of introducing an Internal Heat Exchanger (IHX) to a transcritical CO_2 system operating in the heat pump mode both numerically and experimentally. The results show the efficiency of the IHX HP system is higher than the baseline HP system by up to 11.6% when the heating capacities are identical for both HP systems. Also, the evaporating temperature of the IHX HP system can be higher than it is for the baseline HP system by up to 2.3℃ when the outdoor air temperature is 0℃. In conclusion, introducing IHX helps improve the efficiency of the CO_2 HP system and has considerable benefits for the performance in frosting conditions.

Besides, researchers proposed different active defrosting methods, like reverse cycle defrosting. For reverse cycle defrosting, the indoor heat exchanger works as an evaporator and absorbs heat from indoor air/ heater, while the hot refrigerant is pumped to the outdoor heat exchanger to melt the frost. Payne and O'Neal (1995) experimentally studied the frost accumulation and defrost cycle of a 10.6 kW air-source residential heat pump with the original scroll compressor and a reciprocating compressor. The frosting conditions were 1.7℃ outdoor air temperature and 0.5℃ dew point. The reverse cycle defrosting was initiated at a 20% drop in heat capacity and terminated when the temperature of the lowest liquid line of the outdoor coil reached 26.7℃. The results showed that the low-efficient reciprocating compressor produced 18% higher discharge superheat and thus defrost 5% faster than the scroll compressor with a similar capacity. Wenju et al. (2011) presented an experimental study on the performance of a novel Thermal Energy Storage (TES) based reverse-cycle defrosting method for air-source heat pumps. The results showed the new method reduced the defrosting time by approximately three minutes (38%) and minimized the risk of system shut down due to low suction pressure. In addition, the new method increased the mean indoor coil surface temperature by about 25℃. Dong et al. (2012) conducted experiments to study the defrosting energy supplies and consumptions during a reverse cycle defrosting of an air-source heat pump. During the defrosting, the indoor fan was switched on to provide adequate heat. The data showed that the indoor air provides 71.8% of the total heat supplied for defrosting and 59.4% of the supplied energy was used for melting frost. Also, the maximum defrosting efficiency (energy required to melt the frost and vaporize the retained melted frost/ energy supplied to the outdoor coil) could be up to 60.1%.

Although reverse cycle defrosting has been widely applied for residential ASHP systems with tube-fin heat exchangers, the studies for automobile ASHP systems with microchannel heat exchangers are relatively rare. Steiner and Rieberer (2013) investigated the defrosting performance of an automobile CO_2 heat pump system both experimentally and numerically. The data showed that the defrosting took less than 2 minutes with reverse cycle defrosting, and the final refrigerant inlet temperature of the outdoor coil reached 50℃. The transient simulation results indicate that there is an optimal throttle opening regarding defrosting time and efficiency for the test conditions. The authors emphasized avoiding non-uniform defrosting, where frost-free areas result in heat losses to the ambient, thus increasing the defrost time and reducing defrost efficiency. Li et al. (2021) experimentally studied the benefits of liquid extraction in microchannel condenser using a R134a mobile AC system. The results show a improved COP of the AC system with the extraction-mode condenser than the baseline system with same superheat and same cooling capacity. Zhang and Hrnjak (2021) experimentally studied the effects of different defrost-start criteria on the efficiency and frost accumulation of an automobile CO_2 heat pump during periodic frosting and

reverse cycle defrosting. The frosting condition in this study is the most demanding condition for ASHPs- 0°C and 90% relative humidity. The data showed that the heating capacity and efficiency of the HP drop less than 10% when the air-side pressure drop reaches 5 times of the initial value. Thus, the system can operate longer time by allowing a higher air-side pressure drop. Also, the frosting time increases from 28 to 64 minutes and the percentagewise defrosting time drops from 7.2% to 5.7%, when the criterion changes from 5 to 10 times of the initial air-side pressure drop. The 64-minute operating time of HP is longer than the average commuting time of Americans, so the defrosting can be conducted while the vehicle is parking or charging and the effects on thermal comfort can be eliminated.

In this work, we studied the effects of the orientation of the outdoor microchannel evaporator on the performance of a transcritical CO_2 heat pump during periodic frosting and defrosting. The refrigerant migration, heating capacity, efficiency degradation during the frosting process, and the water retention after defrosting process are presented and discussed. The frosting and defrosting processes were monitored using three web cameras to better understand the refrigerant distribution and frost distribution of the two-pass outdoor coil. The frost accumulation, meltwater drainage, and retention are also measured and analyzed.

2. EXPERIMENTAL SETUP

2.1 Facility

In this paper, a reversible CO_2 heat pump system with microchannel heat exchangers was applied. The system is composed of a one-slab two-pass microchannel outdoor coil, a two-slab four-pass microchannel indoor coil, an integrated Internal Heat Exchanger (IHX) and accumulator (Acc), a semi-hermetic reciprocating compressor, two Electronic Expansion Valves (EXVs), and 6 ball valves. The schematics of the system in both AC/defrosting and HP modes were presented in our previous paper (Zhang and Hrnjak, 2021). The dimension of the key components as well as the details of the sensors were also reported in the paper. In the previous paper, we focused on the effects of the defrost-initiation criteria on system performance, while the effects of the orientation of the outdoor microchannel heat exchanger were studied in this paper. Figure 1 shows the vertically and horizontally installed outdoor microchannel heat exchanger, where the blue/red arrows represent the refrigerant flow directions in HP/defrost modes, and the white arrows represent the airflow directions.

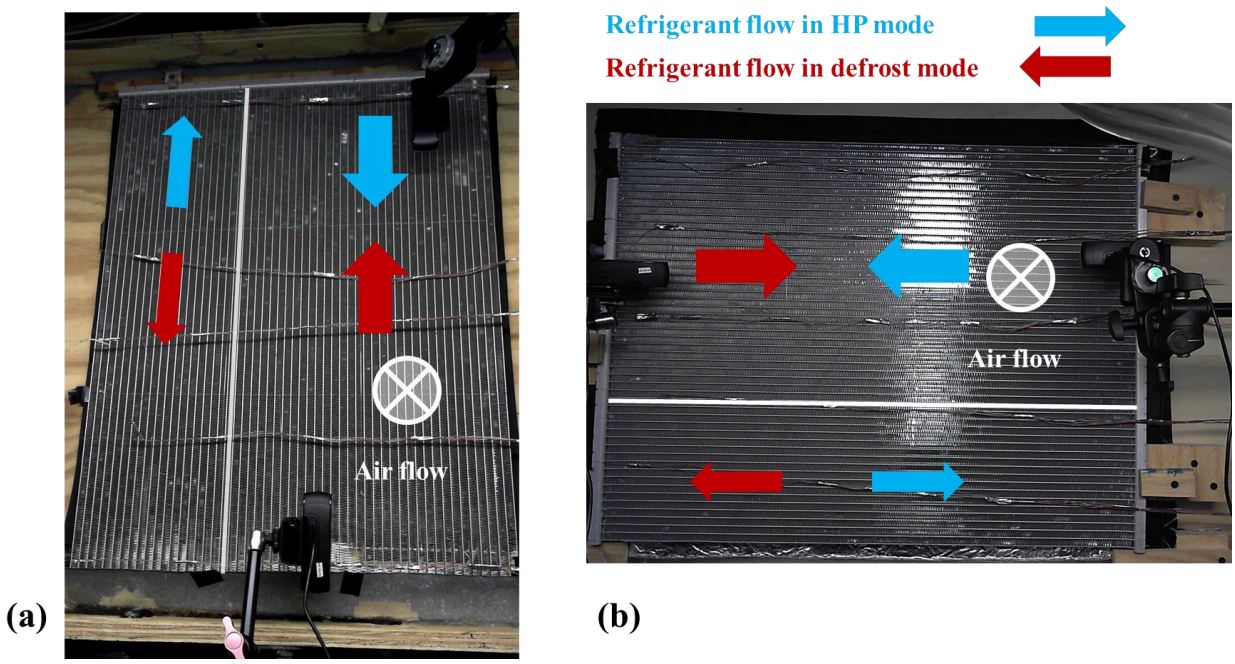

Figure 1: The same outdoor microchannel heat exchanger installed (a) vertically and (b) horizontally: 17 tubes in 1st pass and 34 tubes in 2nd pass

2.2 Experimental procedures and data reduction

The performance of the reversible CO_2 heat pump system in periodic frosting/ defrosting cycles was studied with several steps: frosting, defrosting by reversing the system, water collection, and repeat for periodic performances. The capacities of the heat exchangers were calculated using both air- and refrigerant-side measurements based on the average recording of two minutes. The frost accumulation was calculated based on the air-side measurements of flow rate, dry-bulb temperatures, and dew points. The details of the procedure, the data reduction, and the uncertainty analysis were also presented in our previous paper (Zhang and Hrnjak, 2021). Please note that the defrosting was started when the air-side pressure drop reached 10 times the initial value and terminated when the refrigerant exit temperature of the outdoor gas cooler T_{cro} reached 45 ˚C (Table 1). This defrost-start criterion is chosen due to the assumption that the initiation of the defrost comes from the DP sensor. Nevertheless, the adequacy of the criterion of 10 times initial DP_{ea} is still questionable and will be discussed later, regarding the reduction in the heating capacity and efficiency.

Table 1 shows the operating conditions of the frosting/defrosting experiments in this paper. Especially, 0℃ and 90% RH is the most concerning condition considering the operating time of the heat pump system. On one hand, for the outdoor coil used in this paper, the temperature difference between the inlet air and the evaporating temperature is approximately 2 to 3℃ when the outdoor air velocity is 3 m/s. Thus, the evaporator surface temperature is close to air inlet temperature T_{eai}, and there is no frosting issue when the outdoor air temperature equals to or is higher than 1℃. On the other hand, the absolute humidity drops significantly as the ambient air temperature T_{eai} reduces from 0℃, frost accumulates much slower in colder conditions with the same relative humidity. The other parameters are controlled to simulate a typical driving condition of a vehicle. The number of the frosting/defrosting cycles is limited by the frosting load of the climate control system, in other words, the maximum operating time of the glycol heat exchanger in the outdoor climate chamber while maintaining the outdoor air temperature T_{eai}.

Table 1: Operating conditions of frosting/defrosting experiments

Microchannel tube orientation	T_{eai} [℃]	RH_{ei} [%]	$V_{eai,ini}$ [m/s]	T_{cai} [℃]	U_{cai} [kg/min]	# of frosting cycle	Defrost start criterion	Defrost stop criterion
Vertical	0	90	3.0	20	7.0	1 to 2	10× $DP_{ea,ini}$	T_{cro} = 45 ℃
Horizontal								

3. RESULTS AND DISCUSSION

3.1 Effects of the orientation of outdoor coil during frosting

Figure 2 and Figure 3 show the heating capacity, cooling capacity, air-side pressure drop, compressor work, and the efficiency of the CO_2 heat pump system with vertically and horizontally installed outdoor coil during two continuous frosting and defrosting cycles at 0℃ and 90% RH. The efficiency of the heat pump is defined as the Heating Performance Factor (HPF), which equals the ratio of the heating capacity and the compressor work.

At the beginning of the first frosting cycle, the heating capacities $Q_{heating}$ and the compressor work W_{comp} are identical for the heat pump with vertically and horizontally installed outdoor coil. As a result, the efficiency/ HPF are the same for both orientations. However, the cooling capacity $Q_{cooling}$ of the horizontally installed evaporator is 0.56 kW (+24.9%) higher than that of the vertically installed evaporator. The reason is that the evaporating temperature of the horizontally installed evaporator is lower due to the higher refrigerant-side pressure drop and the less even distribution of the refrigerant. As shown in Figure 4 (a), the refrigerant-side pressure drop across the evaporator DP_{er} is 0.16 bar (+11.9%) higher for the horizontally installed evaporator than it is in the vertical installation. Also, the evaporating temperature is 0.4℃ lower for the horizontally installed evaporator than it is for the vertically installed evaporator (Figure 4 (b)). The evaporator exit refrigerant temperature T_{ero} is used as the evaporating temperature because two-phase refrigerant exits the evaporator during the frosting/defrosting cycles in the test condition. First, the accumulator and IHX were integrated in the HP system. Second, the refrigerant charge amount of the HP system was determined to be 950 g in the condition of the ambient air temperature T_{eai} of 0℃, the ambient relative humidity RH_{ei} of 40%, the outdoor air velocity V_{eai} of 3.0 m/s, the indoor air inlet temperature T_{cai} of 10℃, the indoor air exit temperature T_{cai} of 50℃, and the indoor air mass flow rate U_{eai} of 6.0 kg/min. In this case, two-phase refrigerant exits the outdoor evaporator, of which the heat transfer area is well-utilized in HP mode.

Thus, the air-side pressure drop DP_{ea} of the horizontally installed evaporator increases to the allowed value 12 minutes faster than that of the vertically installed evaporator, since the frost accumulates more quickly. Although the air-side pressure drop is the same at approximately 46 Pa for both orientations at the beginning when the surfaces are dry.

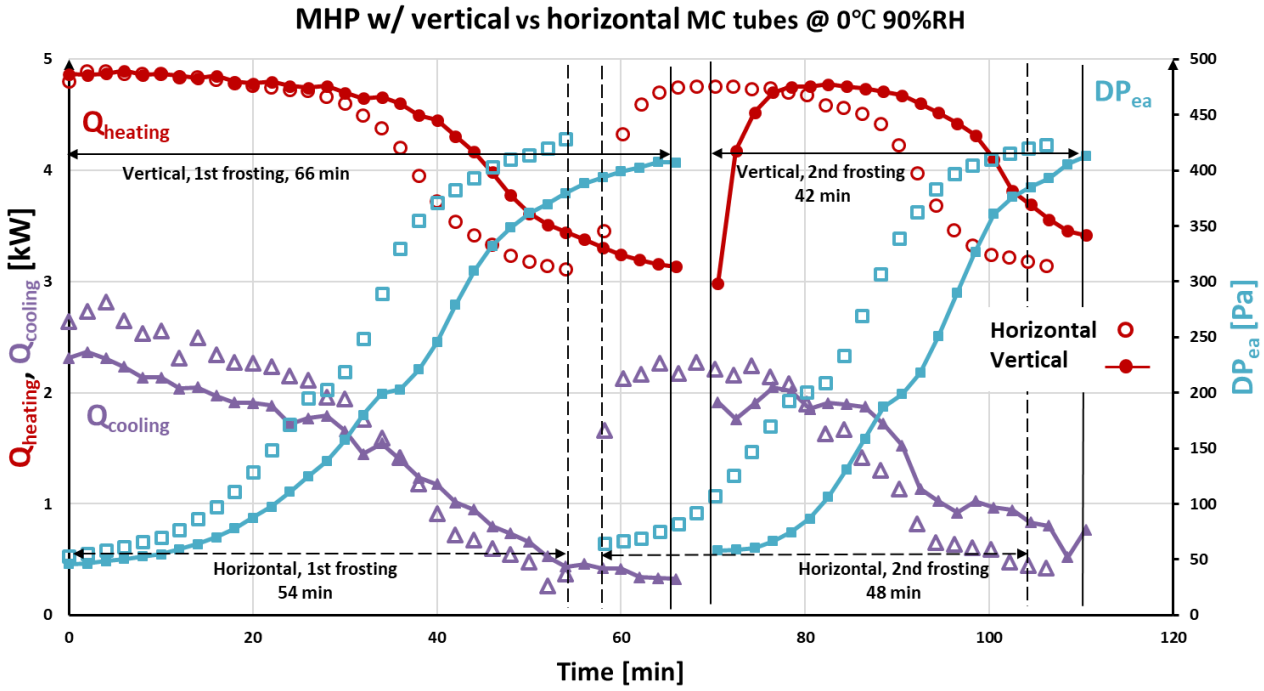

Figure 2: Performance of the CO_2 HP with vertically and horizontally installed outdoor microchannel heat exchanger: the defrosting starts when DP_{ea} reaches 10 times the initial value

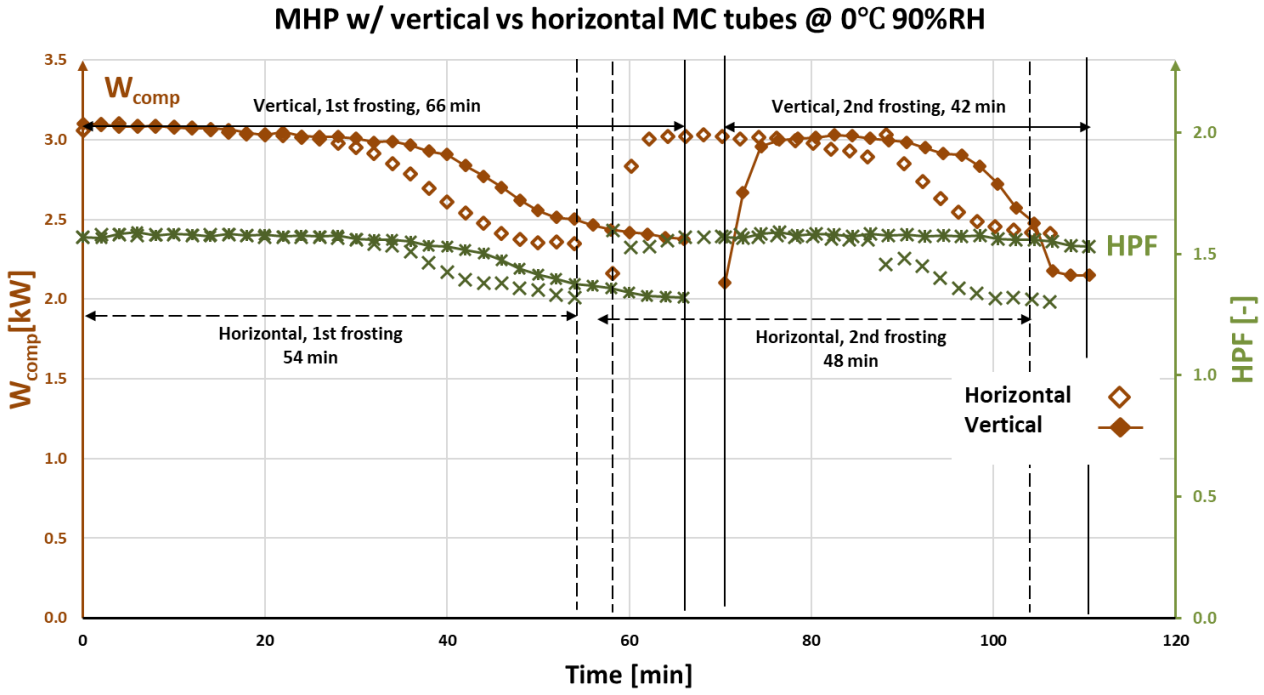

Figure 3: Compressor work and efficiency of the CO_2 HP with vertically and horizontally installed outdoor microchannel heat exchanger: the defrosting starts when DP_{ea} reaches 10 times the initial value

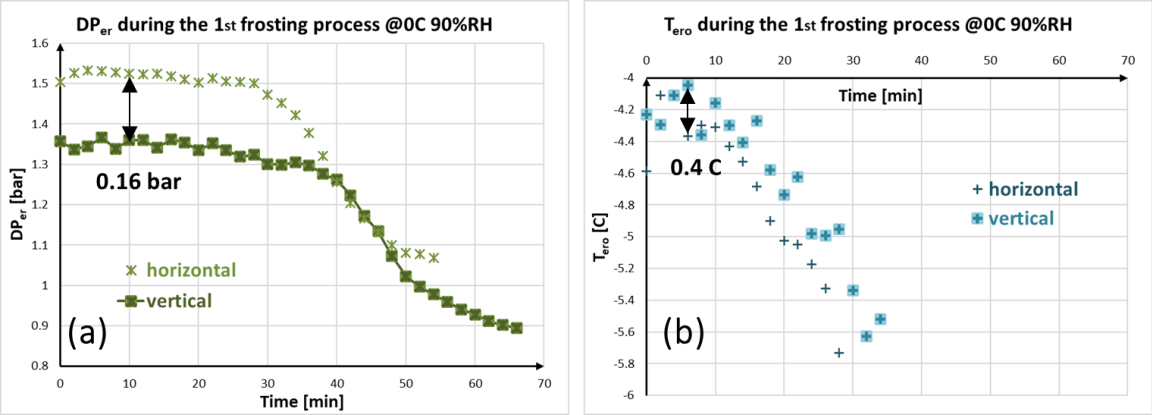

Figure 4: The performance of the vertically and horizontally installed outdoor evaporator: (a) the refrigerant side pressure drop DP_{er} (b) the refrigerant temperature at evaporator exit T_{ero}

Finally, DP_{ea} reaches 10 times the initial value, and defrosting initiates for the heat pump with the horizontally installed evaporator after 54 minutes of operation, which is 12 minutes (-18.2%) shorter than it is for the heat pump with the vertically installed evaporator. Also, by the end of the first frosting cycle, all the parameters in Figure 2 and Figure 3 are identical for both orientations. For example, the heating capacity $Q_{heating}$ drops from 4.89 to 3.12 kW (-35.6 %), and HPF drops from 1.58 to 1.32 (-16.5%) for both vertically and horizontally installed evaporators, even the operating times are different. So, the different orientations only affect the speed of frost accumulation, not the final thermal resistance of the frost. In conclusion, the vertical orientation of the evaporator improves the distribution of the refrigerant, reduces the refrigerant-side pressure drop, and increases the evaporating temperature. Therefore, it prolongs the operating time of the CO_2 heat pump by 12 minutes in the 0℃ and 90% RH ambient condition for the first frosting cycle.

However, the reduction of 35.6% heating capacity and 16.5% efficiency may be seen as relatively mild, considering the time-averaged capacity and efficiency during the operation. Further analysis should indicate whether and when increasing the operating time further, thus increasing the criterion.

The start-up process of the heat pump can be observed at the beginning of the second frosting cycle, which takes about 6 minutes for both orientations. During the start-up, the heating capacity, cooling capacity, and compressor work of the HP system increase but are not able to reach the peak values in the first frosting cycle for both orientations. Also, the air-side pressure drop of the outdoor coil DP_{ea} is approximately 12 Pa higher at the beginning of the second frosting than it is for the first frosting, which indicates water retention after the defrosting.

Then, as frost re-accumulates on the evaporator surface, the performance of the heat pump decreases in a trend similar to the first cycle. The major difference is that the frosting time is shorter for the second frosting cycle. It is 42 minutes for the vertically oriented evaporator and 48 minutes for the horizontally oriented evaporator. However, the heating capacity and HPF of the HP with the vertically oriented evaporator are higher than they are of the HP with the horizontally oriented evaporator by the end of the second frosting. This shows that the HP with vertically installed outdoor coil has the potential to operate longer time- 10 to 12 more minutes based on the data of the first frosting cycle. Thus, air-side pressure drop DP_{ea} might not be the optimal indicator for defrosting initiation. Instead, the heating capacity (gas cooler air exit temperature T_{cao}) or evaporating temperature T_{ero} might be used as the defrosting indicator in the future study.

3.2 Effects of the orientation of outdoor coil on water drainage

Figure 5 presents the mass of frost accumulation on the outdoor evaporator during the operation and the water retention after the defrosting in the 0℃ and 90% RH outdoor condition. During the first 40 minutes of each frosting cycle, the frost accumulates significantly faster than later. The densification of frost happens later at a slower speed. In addition, the frost grows faster on the surface of the horizontally oriented outdoor coil: it accumulates at a rate of 16.7 g/s for the horizontally oriented outdoor coil, while it accumulates at a rate of 12.0 g/s for the vertically oriented outdoor coil. This also supports the previous analysis that the evaporating and surface temperatures of the horizontal evaporator are lower, and frost accumulates faster. Also, the frost accumulation reaches the peak value of

0.64 kg after 40 minutes of operation for the horizontally installed evaporator, while it reaches 0.52 kg after 68 minutes for the vertically installed evaporator. The higher mass of frost for the horizontally installed evaporator might be due to the lower surface temperature and higher frost density.

For the defrost time, it takes 2.6 and 5.2 minutes to defrost the horizontally installed coil in the first and second defrosting cycles. It takes up to 5.2 minutes to melt the frost and warm up a large amount of the retained water (567 g) on the horizontal outdoor coil during the second defrosting so that the refrigerant exit temperature of the outdoor gas cooler reaches the preset value of 45 ˚C. At the same time, it takes 2.5 and 4.0 minutes to defrost the vertically installed coil. Percentage-wise, the defrosting time is 7.0% and 5.6% for horizontally and vertically oriented outdoor coil in the two continuous cycles or approximately two hours of operation.

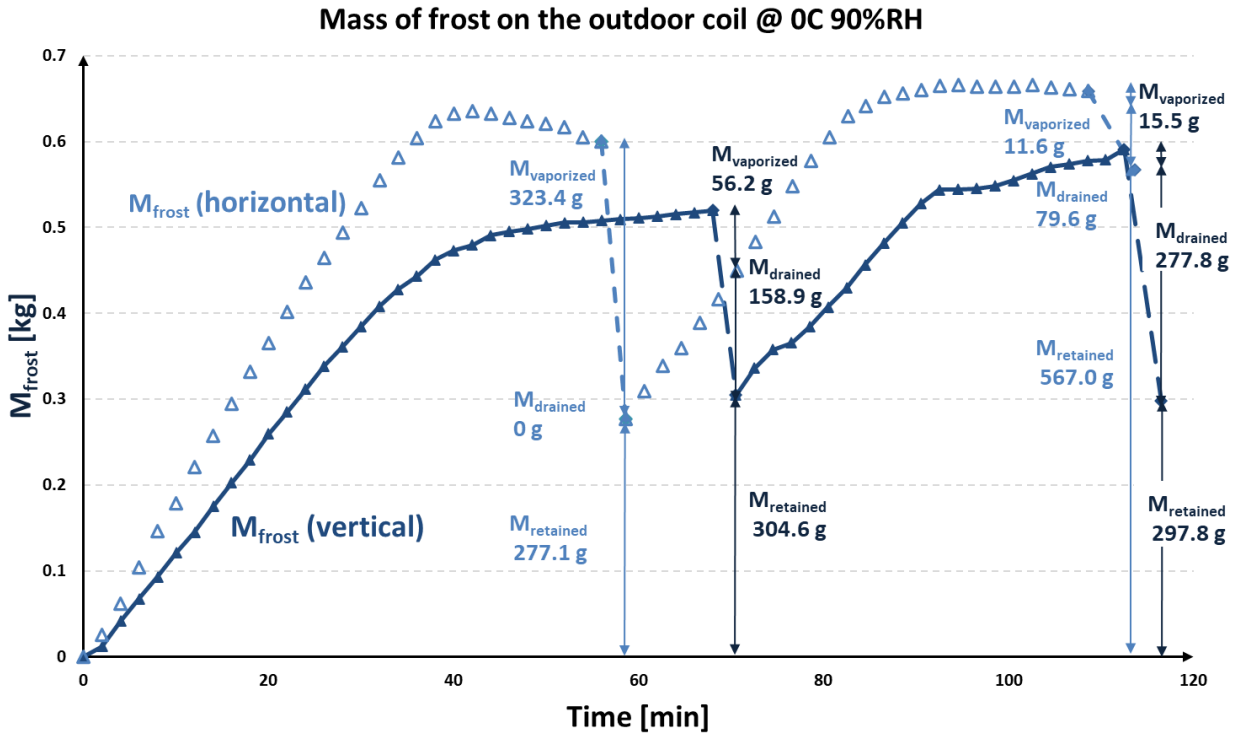

Figure 5: The mass of frost on the vertically and horizontally installed outdoor evaporator

During the defrosting process, the water drainage is much worse for horizontal orientation: the masses of water drainage are 0 and 0.080 kg for the first and second defrosting cycle with the horizontally installed outdoor coil, while it drains 0.159 and 0.278 kg with the vertically installed outdoor coil. In addition, the retained water is 0.277 and 0.567 kg for first and second defrosting with the horizontally installed outdoor coil, while it retains 0.305 and 0.298 kg with the vertically installed outdoor coil. Thus, the vertical outdoor coil gets saturated with retained water of about 0.3 kg, while it can retain at least 0.57 kg of water for the horizontal outdoor coil. In summary, the vertical orientation of the outdoor coil improves the defrosting efficiency by improving the drainage of meltwater.

4. CONCLUSIONS

An R744 air-conditioning system was used to study the effects of outdoor coil orientation on the HP performance during continuous frosting/defrosting cycles experimentally. The results show:

- The operating time of the transcritical HP is longer than 50 minutes in the most demanding ambient condition (0℃ and 90% RH) using the current defrost-start criterion. The operating time is higher than the average commuting time of Americans. This shows the potential to defrost the outdoor coil using the internal energy of indoor air while the car is parking or charging so that the effects on passenger comfort are minimized.

- The operating time could be even longer if we can relax the reduction of 35.6% capacity and 16.5% efficiency by the end of frosting. Further analysis should justify the choice of the defrost-initiation criterion.
- Vertical orientation prolongs the operating time of HP from 54 to 66 minutes (+18.2%). It appears that is because of better refrigerant distribution resulting in a lower refrigerant pressure drop of evaporator DP_{er} for 0.16 bar and the increased evaporating temperature T_{ero} for 0.4℃.
- The outdoor coil in vertical orientation retains 58.7% less water than it does in horizontal orientation after the second defrosting and requires 1.3 minutes shorter defrosting time. Considering the total two-hour operation, vertical orientation reduces the defrosting time from 7.0% to 5.6%.

Overall, the transcritical CO_2 heat pump system with the vertically installed outdoor evaporator has better performance in both frosting and defrosting cycles because of the better distribution of two-phase refrigerant and better water drainage.

NOMENCLATURE

AC	air-conditioning	**IHX**	internal heat exchanger
Acc	accumulator	**M**	mass [kg]
COP	Coefficient of Performance	**P**	pressure [bar]
DP	differential pressure [Pa or bar]	**Q**	capacity [kW]
EXV	electronic expansion valve	**T**	temperature [℃]
h	enthalpy [kJ/kg-℃]	**V**	velocity [m/s]
HP	heat pump	**W**	power [kW]
HPF	Heating Performance Factor		

Subscript

a/ air	air-side	i	inlet
acc	accumulator	g	glycol
c	Condenser/ gas cooler	n	nozzle
cp/ comp	compressor	o	outlet
e	evaporator	r/ ref	refrigerant-side
elec	electricity	x	expansion valve
high	high-pressure side		

REFERENCES

Cernicin, V., Zhang, W., & Hrnjak, P. (2022). The role of internal heat exchanger in an R744 vapor compression system in heat pump mode under various conditions. *International Refrigeration and Air Conditioning Conference.*, No.2153.

Dong, J., Deng, S., Jiang, Y., Xia, L., & Yao, Y. (2012). An experimental study on defrosting heat supplies and energy consumptions during a reverse cycle defrost operation for an air source heat pump. *Applied Thermal Engineering*, *37*, 380–387. https://doi.org/10.1016/j.applthermaleng.2011.11.052

Hayashi, Y., Aoki, A., Adachi, S., & Hori, K. (1977). Study of frost properties correlating with frost formation types. *Journal of Heat Transfer*, *99*(2), 239–245. https://doi.org/10.1115/1.3450675

Hrnjak, P., Zhang, P., & Rennels, C. (2017). Effect of louver angle on performance of heat exchanger with serpentine fins and flat tubes in frosting: Importance of experiments in periodic frosting. *International Journal of Refrigeration*, *84*, 321–335. https://doi.org/10.1016/j.ijrefrig.2017.08.002

Li, J., Muncan, V., Wang, D., & Hrnjak, P. (2021). Experimental Confirmation Of Improvement Of Microchannel Condensers By Extraction Circuitry Using R134a. *International Refrigeration and Air ConditioningConference*. Paper 2194.

Na, B., & Webb, R. L. (2003). A fundamental understanding of factors affecting frost nucleation. *International Journal of Heat and Mass Transfer*, *46*(20), 3797–3808. https://doi.org/10.1016/S0017-9310(03)00194-7

Payne, V., & O'Neal, D. L. (1995). Defrost cycle performance for an air-source heat pump with a scroll and a

reciprocating compressor. *International Journal of Refrigeration*, *18*(2), 107–112. https://doi.org/10.1016/0140-7007(95)93893-O

Steiner, A., & Rieberer, R. (2013). Parametric analysis of the defrosting process of a reversible heat pump system for electric vehicles. *Applied Thermal Engineering*, *61*(2), 393–400. https://doi.org/10.1016/j.applthermaleng.2013.07.044

Wenju, H., Yiqiang, J., Minglu, Q., Long, N., Yang, Y., & Shiming, D. (2011). An experimental study on the operating performance of a novel reverse-cycle hot gas defrosting method for air source heat pumps. *Applied Thermal Engineering*, *31*(2–3), 363–369. https://doi.org/10.1016/j.applthermaleng.2010.09.024

Yang, D. K., & Lee, K. S. (2004). Dimensionless correlations of frost properties on a cold plate. *International Journal of Refrigeration*, *27*(1), 89–96. https://doi.org/10.1016/S0140-7007(03)00118-X

Zhang, P., & Hrnjak, P. S. (2009). Air-side performance evaluation of three types of heat exchangers in dry, wet and periodic frosting conditions. *International Journal of Refrigeration*, *32*(5), 911–921. https://doi.org/10.1016/j.ijrefrig.2008.11.006

Zhang, W., & Hrnjak, P. (2021). The Performance of an Automotive Carbon Dioxide Heat Pump System in Frosting and Defrosting. *18th International Refrigeration and Air Conditioning Conference at Purdue*.

ACKNOWLEDGEMENT

This work was supported by all members of ACRC at the University of Illinois at Urbana-Champaign. All the help from our members is gratefully acknowledged!